A Comparison of Ground- and Excited-State Properties of $[Ru(bz)_2]^{2+}$ and bis(η^6-Benzene)ruthenium(II) *p*-Toluenesulfonate Using the Density Functional Theory

F. GILARDONI,[1] J. WEBER,[1] A. HAUSER,[1] C. DAUL[2]

[1] *Département de Chimie Physique, Université de Genève, 30 Quai Ernest-Ansermet, CH-1211 Genève 4, Switzerland*

[2] *Institut de Chimie Inorganique et Analytique, Université de Fribourg, Pérolles, CH-1700 Fribourg, Switzerland*

Received 21 December 1998; accepted 6 April 1999

ABSTRACT: The ground- and excited-state properties of both $[Ru(bz)_2]^{2+}$ and crystalline bis(η^6-benzene)ruthenium(II) *p*-toluenesulfonate are investigated using the density functional theory. A symmetry-based technique is employed to calculate the energies of the multiplet structure splitting of the singly excited triplet states. For the crystalline system, a Buckingham potential is introduced to describe the intermolecular interactions between the $[Ru(bz)_2]^{2+}$ system and its first shell of neighbor molecules. The overall agreement between experimental and calculated ground- and excited-state properties is good, as far as the absolute transition energies, the Stokes shift, and the geometry of the excited states are concerned. The calculated *d-d* excitation energies of the isolated cluster are typically 1000–2000 cm^{-1} too low. An energy lowering is obtained in $a_{1g} \rightarrow e_{1g}(^3E_{1g})$ excited state when the geometry of $[Ru(bz)_2]^{2+}$ is bent along the e_{1u} Renner–Teller active coordinate. It vanishes as the crystal packing is taken into account. © 1999 John Wiley & Sons, Inc. J Comput Chem 20: 1343–1353, 1999

Keywords: quantum chemical calculations; photophysical properties; multiplet structure; intermolecular interactions; Jahn–Teller distortion

Correspondence to: J. Weber; e-mail: Jacques.Weber@chiphy.unige.ch

CCC 0192-8651 / 99 / 131343-11

Introduction

The electronic structure of bis-benzene (bis-bz) and bis-cyclopenadienyl (bis-cp) sandwich complexes has been subject of a number of studies over the past decades. The ground state and the lowest excited states of transition metal complexes can be described within a ligand-field approach.[1] Complexes of d^6 ions, resulting in an 18-electron configuration, form particularly stable complexes, such as the famous ferrocene. For the title complex that exhibits D_{6h} symmetry,[2] the electronic ground state is $^1A_1(e_{2g})^4(a_{1g})^2$. The e_{2g} and a_{1g} orbitals correspond to the weakly bonding d_{xy} and $d_{x^2-y^2}$ and to the nonbonding d_{z^2} metal orbitals, respectively. The excited states of a ligand field type lie at somewhat lower energies compared to charge transfer states. In the context of photophysical and photochemical activity of this complex, excited states geometries, in particular of the lowest excited state $^3E_{1g}(e_{2g})^4(a_{1g})^1(e_{1g})^1$, corresponding to the promotion of an electron from the nonbonding d_{z^2} orbital to the antibonding d_{yz} and d_{xz} orbitals, are of interest.

At low temperature, luminescence from the $^3E_{1g}$ state is readily observed in polycrystalline material of tetra-borofluorate salt[3] in the form of a broad unstructured band centered at 16'200 cm^{-1} with a full width at half maximum of 3200 cm^{-1}. At 10 K the lifetime of this state is around 400 μs, at higher temperatures it quickly drops, and above 125 K the luminescence is completely quenched. These are clear indications that there are substantial excited state distortions along the one or more normal coordinates of the chromophore. Of course, the prime candidate for a large distortion is the η^6-($Ru-bz$) bond, because the promotion of an electron from the nonbonding to the antibonding orbitals primarily weakens this bond. Karlen et al.[4] have shown that the photochemical ligand substitution proceeds via an associative mechanism. The transition state has to exhibit a bending of the benzene ligands the substituting ligand located between the sandwich.[3] A simple elongation of the η^6-($Ru-bz$) bond in the excited state would not suffice to create the space required for an easy nucleophilic attack of the incoming ligand. The question is if there is a spontaneous distortion in the excited state along a normal coordinate other than the totally symmetry stretch. Indeed, viewed as a pseudolinear triatomic molecule ($D_{\infty h}$), the excited state has Π_g symmetry and it is susceptible to a Renner–Teller (RT)-type distortion along the π_u bending coordinate, transforming as e_u in D_{6h}. The $e_u(bz-Ru-bz)$ bending coordinate lifts the orbital degeneracy of the $^3E_{1g}$ state. In contrast to the Jahn–Teller case where the active vibration is even, the linear vibronic coupling matrix element is zero, and a large quadratic coupling is required to result in an actual distortion along this coordinate. The aim of the present work is to quantitatively investigate excited-state distortions along both the totally symmetric stretch as well as the above-mentioned bending coordinate using the density functional theory (DFT).

Computational Methods

DENSITY FUNCTIONAL CALCULATIONS

The Hartree–Fock–Slater linear combination of atomic orbitals (HFS-LCAO), as implemented in the Amsterdam density functional (ADF) program system developed by Baerends et al.[4–7] was used. All the calculations reported in this study were performed using the Vosko–Wilk–Nusair (VWN) exchange-correlation potential.[8] The ADF atomic orbitals were described using an uncontracted triple zeta Slater-type orbital basis set on Ru and augmented by single polarization functions on both C and H. The $1s$ shell of carbon and the $1s^2 2s^2 2p^6 3s^2 3p^6 3d^{10}$ shells of ruthenium were assigned to the core and treated using the frozen core approximation.[5] A set of auxiliary s, p, d, f, and g functions, centered on all nuclei,[9] was used to fit electron density, together with both Coulomb and exchange potentials in each self-consistent field (SCF) cycle.

The geometry of gas-phase bis(η^6-benzene)ruthenium(II) ($[Ru(bz)_2]^{2+}$) was taken in its eclipsed conformation[3] (D_{6h} symmetry) in which both the C—C and C—H bond distances were kept frozen in all calculations at 1.414 and 0.919 Å, respectively.[2] The geometry of the crystal was taken from X-ray structure data.[2]

MULTIPLET STRUCTURE

From a purely theoretical point of view, excited states are difficult to handle in the DF theory. The Hohenberg–Kohn theorems[10] are, in principle, valid for a ground-state electron density, and as in any Hartree–Fock-based model, there is the orthogonality problem of the excited state wave

function to the ground state one.[11] However, for a decade, DF models have represented a valuable alternative to traditional configuration interaction (CI) approaches to evaluate the properties of excited states. In addition, local-spin density (LSD) methods provide a similar level of accuracy in describing ground and excited states,[12–14,22] leading to accurate predictions of both structure and properties of organometallic compounds.[15–20]

The calculation of the multiplet splitting in the DF theory has been recently discussed by Ziegler et al.[21] and Daul et al.[22,23,26] According to these authors, it is possible to replace the energy of a single determinant (SD) by the corresponding statistical energy as obtained in the DF theory. The energy of a multiplet arising from a given configuration being a weighted sum of single-determinantal energies, it is thus possible to obtain the multiplet splitting. Following this line of thought, we used symmetry-based arguments to rationalize the relation between the multiplet splitting and the single-determinantal energies resulting from DF calculations. A slightly simplified calculation scheme suggested from Slater's Transition State[24] (TS) method has been used to derive ground- and excited-state energies. It should be pointed out that the TS model has no relation with transition states of chemical reactions. The scheme commonly used, namely delta self-consistent field (ΔSCF), consists of solving the Kohn–Sham (KS) equations for the symmetrically averaged density (SAD) of the configurations, corresponding, respectively, to the ground state and to each excited state in separate SCF calculations. On the other hand, the TS method solves the KS equations self-consistently for the SAD of the reference configurations, namely the transition state, which is located exactly halfway between the ground and the excited-state configuration.

As eclipsed [Ru(bz)$_2$]$^{2+}$ exhibits D_{6h} symmetry, the $4d$ orbitals of ruthenium split into e_{2g}, a_{1g} and e_{1g} components. This $4d^6$ system has the following ground state (GS) configuration

$$\left|(6e_{2g})^4(5a_{1g})^2(7e_{1g})^0\,{}^1A_{1g}\right\rangle.$$

Furthermore, when considering singly excited triplet states only, we have,

$$\left|(6e_{2g})^4(5a_{1g})^1(7e_{1g})^1\,{}^3E_{1g}\right\rangle,$$
$$\left|(6e_{2g})^3(5a_{1g})^2(7e_{1g})^1\,{}^3B_{2g}\right\rangle,$$
$$\left|(6e_{2g})^3(5a_{1g})^2(7e_{1g})^1\,{}^3B_{2g}\right\rangle,$$
$$\left|(6e_{2g})^3(5a_{1g})^2(7e_{1g})^1\,{}^3E_{1g}\right\rangle.$$

Applying the model described by Daul et al.[21,23] the multiplet energies may be expressed as a weighted sum of nonredundant single determinants (NRSD) energies, namely $E(\Phi_i)$. We have,

$$E\left(\left|(6e_{2g})^4(5a_{1g})^2(7e_{1g})^0\,{}^1A_{1g}\right\rangle\right) = E(\Phi_1),$$
$$E\left(\left|(6e_{2g})^4(5a_{1g})^1(7e_{1g})^1\,{}^1E_{1g}\right\rangle\right) = +2E(\Phi_2) - E(\Phi_3),$$
$$E\left(\left|(6e_{2g})^4(5a_{1g})^1(7e_{1g})^1\,{}^3E_{1g}\right\rangle\right) = E(\Phi_3),$$
$$E\left(\left|(6e_{2g})^3(5a_{1g})^2(7e_{1g})^1\,{}^1B_{1g}\right\rangle\right) = +4E(\Phi_4) - 2.5E(\Phi_5) - 2E(\Phi_6) + 1.5E(\Phi_7),$$
$$E\left(\left|(6e_{2g})^3(5a_{1g})^2(7e_{1g})^1\,{}^3B_{1g}\right\rangle\right) = +1.5E(\Phi_5) - 0.5E(\Phi_7),$$
$$E\left(\left|(6e_{2g})^3(5a_{1g})^2(7e_{1g})^1\,{}^1B_{2g}\right\rangle\right) = -0.5E(\Phi_5) + 2E(\Phi_6) - 0.5E(\Phi_6),$$
$$E\left(\left|(6e_{2g})^3(5a_{1g})^2(7e_{1g})^1\,{}^3B_{2g}\right\rangle\right) = -0.5E(\Phi_5) + 1.5E(\Phi_7),$$
$$E\left(\left|(6e_{2g})^3(5a_{1g})^2(7e_{1g})^1\,{}^1E_{1g}\right\rangle\right) = +0.5E(\Phi_5) + 2E(\Phi_6) - 1.5E(\Phi_7),$$
$$E\left(\left|(6e_{2g})^3(5a_{1g})^2(7e_{1g})^1\,{}^3E_{1g}\right\rangle\right) = +0.5E(\Phi_5) + 0.5E(\Phi_7),$$

where the energies $E(\Phi_i)$ are those of the single-determinant wave functions,

$$\Phi_1 = \left|(d_{x^2-y^2})^2(d_{xy})^2(d_{z^2})^2\right|$$
$$\Phi_2 = \left|(d_{x^2-y^2})^2(d_{xy})^2(d_{z^2})^-(d_{xz})^+\right|$$
$$\Phi_3 = \left|(d_{x^2-y^2})^2(d_{xy})^2(d_{z^2})^-(d_{xz})^-\right|$$
$$\Phi_4 = \left|(d_{x^2-y^2})^2(d_{xy})^-(d_{z^2})^2(d_{xz})^+\right|$$
$$\Phi_5 = \left|(d_{x^2-y^2})^2(d_{xy})^-(d_{z^2})^2(d_{xz})^-\right|$$
$$\Phi_6 = \left|(d_{x^2-y^2})^2(d_{xy})^-(d_{z^2})^2(d_{yz})^+\right|$$
$$\Phi_7 = \left|(d_{x^2-y^2})^2(d_{xy})^-(d_{z^2})^2(d_{yz})^-\right|$$

The latter were obtained applying the TS method; + and − refer to spin-up and spin-down spin-orbitals. This method only describes the first-order electrostatic interactions.[20,21] The second-order effects that are neither of Coulomb nor exchange type can be approximated by the ligand-field theory to take into account the CI of the $^3E_1$ excited states. The off-diagonal electrostatic two-electron integrals were expressed[22,25] as,

$$\langle 6e_{2g}5a_{1g}|7e_{1g}7e_{1g}\rangle = -2\sqrt{3}B,$$

where B is the Racah parameter. We estimated $B = 450\ \text{cm}^{-1}$, the free ion value being $474\ \text{cm}^{-1}$. Daul et al.[22] have shown that the value chosen for B is not critical, as modifying it by a factor 2 does not significantly effect the results. Moreover, the CI is expected to be small due to the large energy gap (about $2200\ \text{cm}^{-1}$) between the $^3E_{1g}$ excited states.

POTENTIAL ENERGY STATES

The adiabatic potential energy surfaces of the ground and excited states were calculated along the a_{1g} and the e_{1u} normal modes. The bending model e_{1u} lowers the D_{6h} symmetry to C_{2v} and splits up $^3E_{1g} \rightarrow {}^3B_1 + {}^3B_2$, transforming $^3B_{1g} \rightarrow {}^3B_1$ and $^3B_{2g} \rightarrow {}^3B_2$. We finally have

$$\left|(13a_1)^2(5a_2)^2(14a_1)^2(10b_1)^0(10b_2)^{0\,1}A_1)\right\rangle, \quad \text{(GS)}$$

$$\left|(13a_1)^2(5a_2)^2(14a_1)^1(10b_1)^0(10b_2)^{1\,3}B_2)\right\rangle, \quad (E_1)$$

$$\left|(13a_1)^2(5a_2)^2(14a_1)^1(10b_1)^1(10b_2)^{0\,3}B_1)\right\rangle, \quad (E_2)$$

$$\left|(13a_1)^1(5a_2)^2(14a_1)^2(10b_1)^1(10b_2)^{0\,3}B_1)\right\rangle, \quad (E_3)$$

$$\left|(13a_1)^1(5a_2)^2(14a_1)^2(10b_1)^0(10b_2)^{1\,3}B_2)\right\rangle, \quad (E_4)$$

$$\left|(13a_1)^2(5a_2)^1(14a_1)^2(10b_1)^1(10b_2)^{0\,3}B_2)\right\rangle, \quad (E_5)$$

$$\left|(13a_1)^5(5a_2)^1(14a_1)^2(10b_1)^0(10b_2)^{1\,3}B_1)\right\rangle. \quad (E_6)$$

In the present case, DF calculations can describe both the ground state and these six nondegenerate excited states.[20,23]

INTERMOLECULAR POTENTIAL IN THE CRYSTAL

The crystal structure consists of neutral assemblies of $[Ru(C_6H_6)_2](tos)_2$.[2] The negatively charged SO_3 groups of two tosylate anions point towards two open faces of the hexagonal-prismatic cation with an average Ru—O distance of 4.41 Å. Corresponding nonbonded O—H distances are in the range 2.24–2.58 Å. The benzene rings of the counterion and the coordinates arenas are approximately parallel.

It is well known that, in ionic crystals, the Coulombic interaction between a given cluster and the surrounding lattice may be described using a so-called Madelung potential.[26] Because in preliminary calculations no adequate form of the latter was able to reproduce accurately DF calculations performed on a set of clusters made by $[Ru(bz)_2]^{2+}$ and tosylate anions, we derived a more adequate force field parameterized from DF calculations. For that intricate task, a set of two clusters made of (a) three $[Ru(bz)_2]^{2+}$ molecules [see Fig. 1], and (b) one $[Ru(bz)_2]^{2+}$ surrounded by two tosylate anions (see Figs. 2a and 2b) were used. The position of the neighbors was chosen so as (a) to reduce the computational effort by using a symmetry constraint (C_s, C_{2v}), (b) to keep the same numerical grids and integration accuracy for all calculations, and (c) to have intermolecular distances close to those in the crystal.

We first calculated the potential energy curve of a single $[Ru(bz)_2]^{2+}$ as a function of its bending angle α defined as the angle between the two ligand rings. The calculations was repeated by adding the two neighboring molecules (see Figs. 1, 2a, and 2b), keeping their geometry frozen.

We then expressed the resulting interacting energy $E^{\text{tot}}_{\text{clu}}(\alpha)$, as

$$E^{\text{int}}_{\text{clu}}(\alpha) = E^{\text{tot}}_{\alpha}(\text{cluster}) - E^{\text{tot}}_{\alpha}(\text{single}) - E^{\text{tot}}_{\alpha=0}(\text{neighbors}), \quad (1)$$

where E^{tot}_{α}(cluster) is the total energy of the cluster, E^{tot}_{α}(single) is the total energy of a single bent $[Ru(bz)_2]^{2+}$ and $E^{\text{tot}}_{\alpha=0}$(neighbors) is the energy of

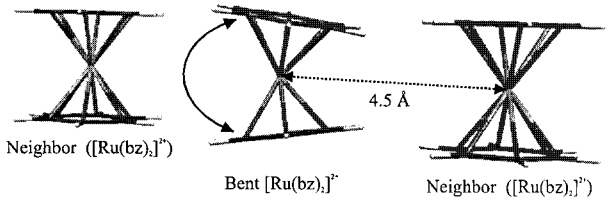

FIGURE 1. Cluster made of three $[Ru(bz)_2]^{2+}$. The central $[Ru(bz)_2]^{2+}$ is relaxed along one mode of the normal coordinate e_{1u}. The geometry of the neighbors is kept frozen during all the calculations.

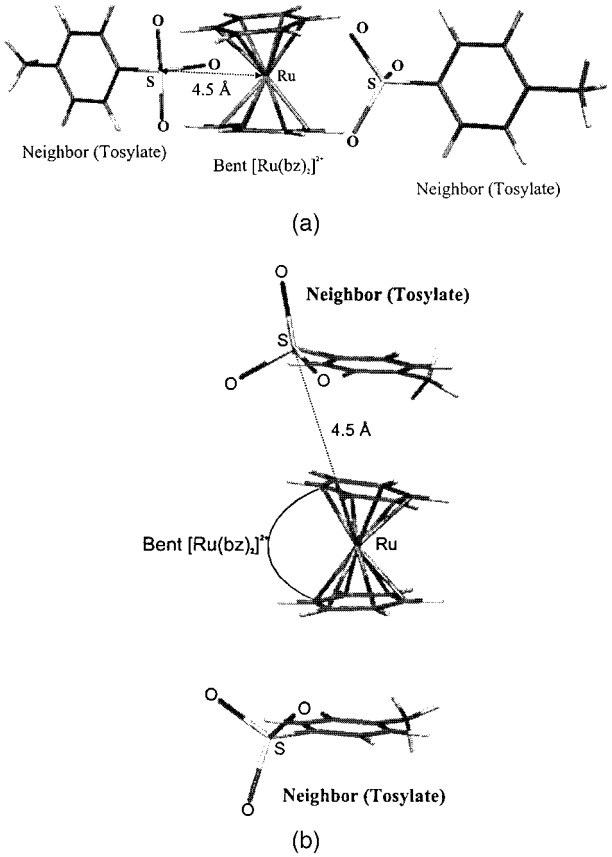

FIGURE 2. (a) As in Figure 1, but the cluster is made of a $[Ru(bz)_2]^{2+}$ surrounded by a set of two tosylate anions. (b) As in Figure 2a, but with a different arrangement.

the neighbors, calculated for unbent molecules ($\alpha = 0$).

The next step was to derive an intermolecular potential by fitting accurately $E_{clu}^{tot}(\alpha)$ obtained from DF calculations. A fit of $E_{clu}^{int}(\alpha)$ to a Buckingham potential[27] (BUP) led to the best agreement with a root-mean-square (RMS) error of 15 cm^{-1} with respect to DF values. The BUP was already introduced successfully for the modeling of the crystal packing of crystalline ruthenocene.[20] The potential has been defined as (eV units),

$$E_{clu}^{int} = \sum_i \sum_j A \cdot e^{-B \cdot r_{ij}} - \frac{C}{r_{ij}^6}, \qquad (2)$$

where,

$$A = 20.14 \cdot \sqrt{(\varepsilon_i \cdot \varepsilon_j)}, \qquad (3)$$

TABLE I.
Nonbonded Interaction Parameters in Buckingham Potential Used in Eq. (2). (Units: eV and Å).

Element	Adjusted Parameter ε [d]	Van der Waals Radius
C[a]	0.0280	1.90
H[a]	0.0276	1.44
O[a]	0.0090	1.70
S[a]	4.311	2.00
C[b]	0.3545	1.90
H[b]	0.4999	1.44
Ru[c]	0.0000	2.20

[a] In tosylates.
[b] In $[Ru(bz)_2]^{2+}$.
[c] Not taken into account.
[d] Parameters ε are adjusted in order to fit DF results.

$$B = \frac{12.50}{(R_i - R_j)}, \qquad (4)$$

$$C = \frac{2.55 \cdot \sqrt{(\varepsilon_i \cdot \varepsilon_j)} \cdot (R_i + R_j)^6}{144}. \qquad (5)$$

R_i is the van der Waals radius of atom i and r_{ij} the distances between atoms of the central $[Ru(bz)_2]^{2+}$ and those of its first shell of neighbors j. Parameters ε_k were fitted to DF results. The values of these parameters are displayed in Table I.

The fit function of eq. (2) was used in to calculate $E_{shell}^{int}(\alpha)$ between a single $[Ru(bz)_2]^{2+}$ and its first shell of neighbors located at their positions in the crystal.[2] This led to a cluster made of $6[Ru(bz)_2]^{2+}$ and 10 tosylates anions, as shown in Figure 3. The local symmetry of $[Ru(bz)_2]^{2+}$ is lowered in the crystal by the surrounding, as displayed in Figure 4a. Because the discrepancy between the two components of e_{1u}, namely Q_ε and Q_θ, is small on the first order (see Fig. 4b), $E_{shell}^{int}(\alpha)$ may be averaged on all normal coordinates of the bending mode. The overall displacement Q is equivalent to a precession movement around the C_6 axis of $[Ru(bz)_2]^{2+}$, and may be then expressed as a function of Q_ε and Q_θ,

$$Q_\varepsilon = Q\cos(\phi) \qquad \text{with } \phi = 0, \ldots, 2\pi, \qquad (6)$$

$$Q_\theta = Q\sin(\phi) \qquad \text{with } \phi = 0, \ldots, 2\pi, \qquad (7)$$

where ϕ is the precession angle, in the σ_h plane of $[Ru(bz)_2]^{2+}$.

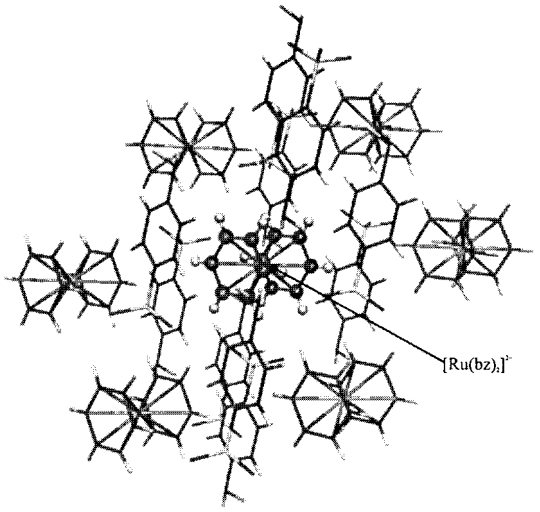

FIGURE 3. First shell of neighbors located at their positions in the crystal used to model the crystal lattice. The central $[Ru(bz)_2]^{2+}$ is surrounded by 6 $[Ru(bz)_2]^{2+}$ and 1 tosylate anions.

Results and Discussion

GROUND AND EXCITED-STATES STRUCTURES

The vertical metal-ring distance in metallocenes, particularly in ferrocene, is a structural parameter that is very difficult to reproduce by *ab initio* quantum chemical calculations.[22,28–30] It was, therefore, of particular interest to optimize the d(Ru–bz) distances of both the ground and the triplet excited states using the present HFS-LCAO-DF model. The results are displayed in Table II. The latter shows the good agreement between the calculations and the X-ray structure data, the predicted ground state d(Ru–bz) distance being only +0.012 Å longer than the 1.717 Å experimental result. The consistency of LDA calculations was checked by expanding the level of approximation. This was achieved by using the VWN[8] exchange-correlation functional augmented by nonlocal gradient correction, as suggested by Becke[31] for exchange and Perdew[32] for correlation (Be88–P86). Table II shows that the Be88–P86 functional increases the metal–ligand bond length by roughly +0.044 Å and +0.096 Å for $^1A_{1g}$ and $^3E_{1g}$, respectively. However, contractions of the same order of magnitude are expected by including relativistic effects,[33–39] yielding to bond lengths close to those obtained by LDA.

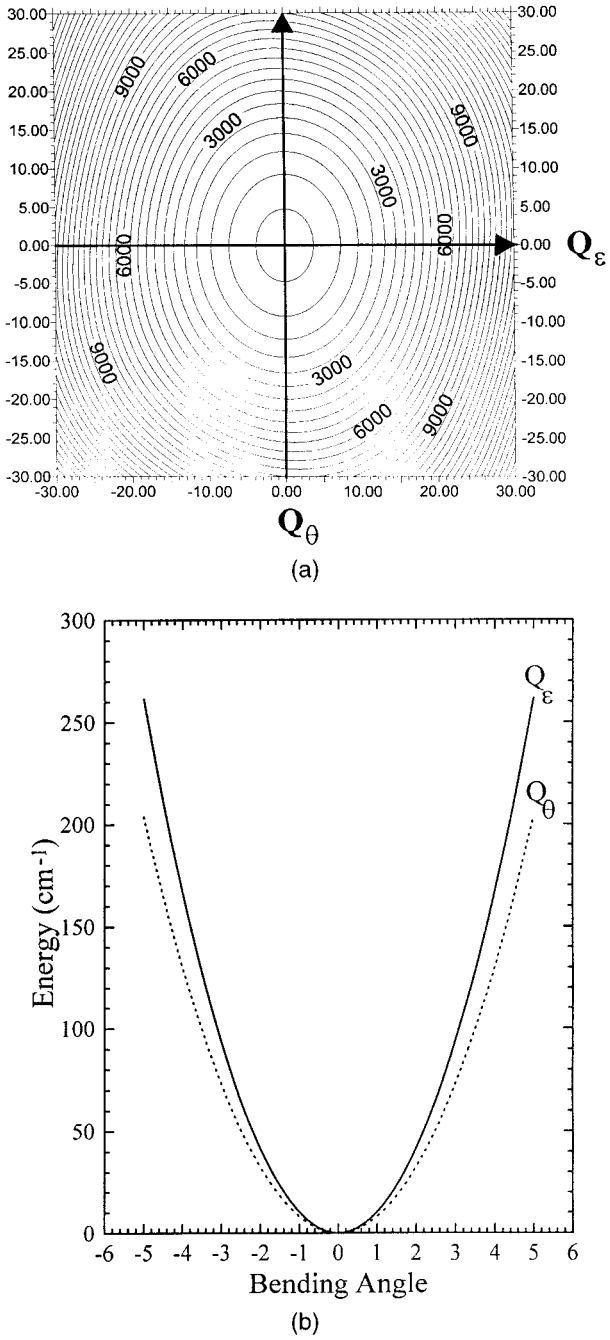

FIGURE 4. (a) Potential energy surface calculated along the two components (Q_ε and Q_θ) of e_{1u} in the solid state. (b) Potential energy curves calculated along the two components (Q_ε and Q_θ) of e_{1u} in the solid state. The local symmetry of $[Ru(bz)_2]^{2+}$ is lowered in the crystal by the surroundings. At the first order, the total contribution can be averaged on Q_ε and Q_θ.

The structure of $[Ru(bz)_2]^{2+}$ is significantly expanded (+0.121 Å) in the triplet excited state, corresponding to a promotion of an electron to the strongly antibonding e_{1g} orbital. The expansion is

TABLE II.
Comparison between Experimental and Calculated Ground- and Excited-State Properties of bis(η^6-Benzene)ruthenium(II) *p*-Toluenesulfonate (C) and (G) $[Ru(bz)_2]^{2+}$.

	Calculated	Experiment
$^1A_1 \rightarrow {}^3E_1$	20 850 cm^{-1}(G)(18 250 cm^{-1})	22000 cm^{-1}[a]
absorption maximum	21 270 cm^{-1}(C)(18 790 cm^{-1})	
$^3E_1 \rightarrow {}^1A_1$	14 100 cm^{-1}(G)(15 100 cm^{-1})	16200 cm^{-1}[a]
emission maximum	15 900 cm^{-1}(C)(16 990 cm^{-1})	
Stokes shift	6 750 cm^{-1}(G)(3 150 cm^{-1})	5800 cm^{-1}[a]
	5 370 cm^{-1}(C)(1 800 cm^{-1})	
d(Ru−bz)in	1.729 Å(G)(1.773 Å)	1.717 Å[b]
$\|(6e_{2g})^4(5a_{1g})^2(6e_{1g})^0 {}^1A_{1g}\rangle$	1.720 Å(C)(1.762 Å)	
Stretching $a_{1g}\|{}^1A_{1g}\rangle$	306 cm^{-1}(G)(314 cm^{-1})	—
	318 cm^{-1}(C)(327 cm^{-1})	
Bending $e_u\|{}^1A_{1g}\rangle$	143 cm^{-1}(G)(148 cm^{-1})	—
	—	
d(ru−bz)in	1.850 Å(G)(1.946 Å)	—
$\|(6e_{2g})^4(5a_{1g})^1(6e_{1g})^1 {}^3E_{1g}\rangle$	1.828 Å(C)(1.922 Å)	
α(bz-Ru-bz)in	±20° (G)(±17°)	—
$\|(6e_{2g})^4(5a_{1g})^1(6e_{1g})^1 {}^3E_{1g}\rangle$	0° (C)(0°)	—
Renner−Teller stabilization in	630 cm^{-1}(G)(310 cm^{-1})	—
$\|(6e_{2g})^4(5a_{1g})^1(6e_{1g})^1 {}^3E_{1g}\rangle$	0 cm^{-1}(C)(0 cm^{-1})	—
Stretching $a_{1g}\|{}^3E_{1g}\rangle$	237 cm^{-1}(G)(245 cm^{-1})	—
	268 cm^{-1}(C)(277 cm^{-1})	
f(GS)/*f*(ES)	1.66(G)(1.64)	—
	1.41(C)(1.39)	

Nonlocal values are in parentheses.
[a] From ref. 3.
[b] From ref. 2.

slightly larger (+0.135 Å) for the successive singly excited triplet states, namely $^3B_{1g}$, $^3B_{2g}$, and $^3E_{1g}$.

Figure 5 displays the adiabatic potential of both the $^1A_{1g}$ and $^3E_{1g}$ states in the gas phase, along the totally symmetric a_{1g} stretch metal-ring stretch. Their vibrational frequency are 306 cm^{-1} and 237 cm^{-1}, respectively, and they were calculated on the basis of a reduced mass equivalent to the full ligand mass of the benzene rings. The nonlocal values are slightly larger (314 cm^{-1} and 268 cm^{-1}).

The adiabatic potentials were calculated for both the $^1A_{1g}$ and the singly excited triplet states (see Fig. 6) along one component of the e_{1u} δ(bz−Ru−bz) bending mode. The excited-state bending will be extensively discussed in the Excited State Bending section. Again, the total mass of the benzene ring was used as the reduced mass for calculating the vibrational frequency, estimated to 143 cm^{-1} for the ground state (nonlocal 148 cm^{-1}).

On the adiabatic potential along the a_{1g} metal-ring stretch, the effect of the crystal packing is to slightly shorten the *d*(Ru−bz) distance, as displayed in Table II. The $^1A_{1g}$ state has its metal-ring bond length reduced by 0.009 Å, leading to an excellent agreement (+0.003 Å) between the calculations and the X-ray diffraction data. Because the steric hindrance of the neighboring atoms drastically grows as the metal-ring distance increases, the latter is largely shortened as the singly excited states are concerned (−0.022 Å). Unfortunately, the structural parameters of the $^3E_{1g}$ excited state are unknown, and no comparisons with the experiment can be made. Concerning the vibrational frequencies, an increase of roughly 10 cm^{-1} is observed for both ground and excited states as the Buckingham potential is included.

Finally, one might wonder why our DFT structural prediction of the metal-ring distance using a local potential is in good agreement with the experiment. One might argue that a similar level of accuracy has been obtained for ruthenocene under the same level of approximation,[22] which seems to

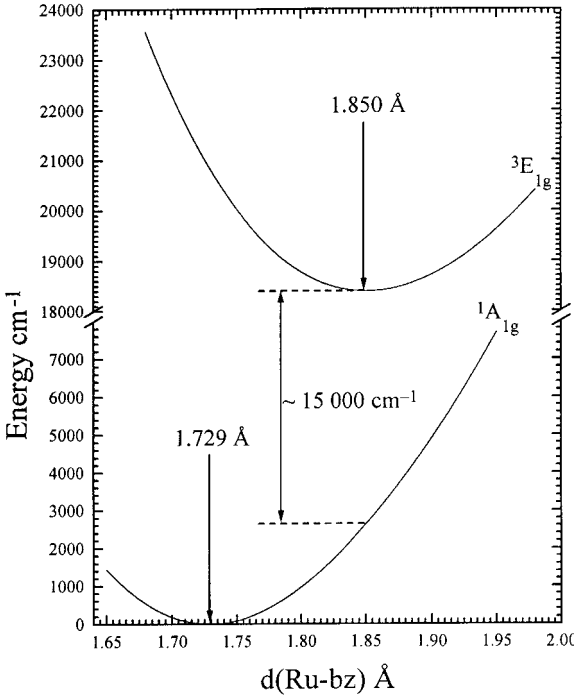

FIGURE 5. Adiabatic potential of both the ground state and the first singly excited triplet state in the gas phase along the totally symmetric a_{1g} metal-ring stretch.

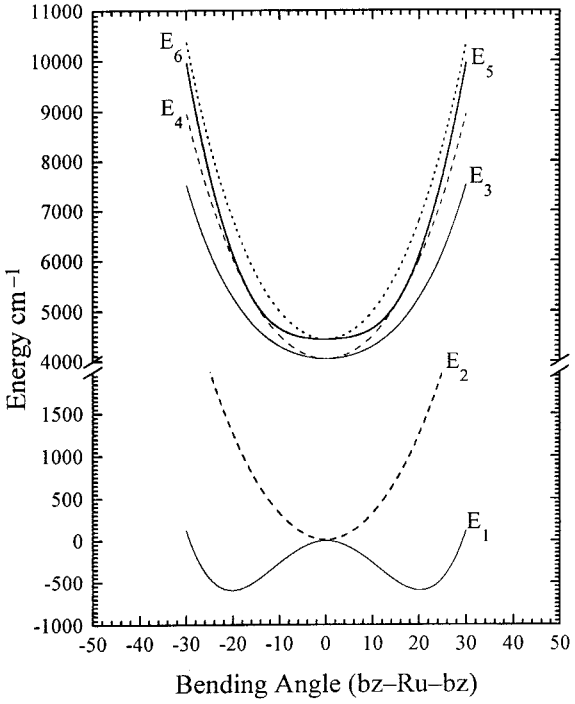

FIGURE 6. Adiabatic potential of the six singly excited triplet states in the gas phase along the Q_ε component of the e_{1u} δ(bz–Ru–bz) bending vibration. The $^3B_2$ [see E_1] is Renner–Teller active. The stabilization energy is about 650 cm^{-1}.

indicate that local potentials are adequate for those systems.

ELECTRONIC EXCITATIONS ENERGIES

Accurate experimental values[3] of the excited-state energies are displayed in Table II. Both the calculated absorption and the emission maxima, i.e., the energies in a configurational coordinate diagram of the Franck–Condon transitions of $^1A_{1g} \leftrightarrow {}^3E_{1g}$, come out slightly smaller than the experimental values (~ -1500 cm^{-1}). This is true for both $[Ru(bz)_2]^{2+}$ and bis(η^6-benzene)ruthenium(II) *p*-toluenesulfonate. The BUP corrects the transition energies in the right direction ($\sim +1100$ cm^{-1}), but its magnitude is not sufficient to get a perfect concordance with the experimental values. The absorption energies are about 1150 cm^{-1} too low, and the discrepancy increases up to -1900 cm^{-1} for the emission. The inclusion of BUP corrects the absorption energies only slightly ($\sim +400$ cm^{-1}), while it drastically increases the emission (the Renner–Teller energy is already taken into account) energy by around 1800 cm^{-1}. Again, the present calculations show that DFT is a reliable tool for predicting structural and photochemical properties of organometallic compounds.[20, 22, 23, 26]

The inclusion of second-order electrostatic interaction approximated by the ligand-field theory[22] leads to similar results. Another problem inherent to the TS method is the redundancy condition of the single determinants, which is not fulfilled in general.[40] This is probably related to the approximate description of the exchange interaction in practical DF calculations. In the cases of atomic multiplet calculations, there are errors reported for the energies of redundant single determinants as large as several thousands wave numbers. Commonly, the magnitude of the deviation never exceeds several wave numbers, and the overestimation of the photochemical properties has to be found elsewhere.

The Stokes shift of the $^1A_{1g} \rightarrow {}^3E_{1g}$ transition is another critical test for our calculations. The overall agreement is good. The local approximation overestimates the Stokes shift by roughly $+950$ cm^{-1}. The inclusion of the BUP reduces the discrepancy to -430 cm^{-1}. On the other hand, the nonlocal values are far from experiment. Again,

the combination of local calculations and the Buckingham potential for the modeling of the crystal packing leads to a good agreement with experiment.

Let us conclude with the transition $6e_{2g} \rightarrow 7e_{1g}$. The energy ordering of the corresponding excited states is $^3B_1 < ^3E_1 < ^3B_2$, and their energies increase regularly by 300 cm^{-1}. The energy gap between the latter one and the first $^3E_1$ is about 2500 cm^{-1}.

EXCITED-STATE BENDING

A particular characteristic of the title compounds lies in the fact that the $^3E_{1g}$ state is susceptible to a Renner–Teller effect along e_{1u}. As mentioned above, the RT effect describes the vibronic coupling involving orbitally degenerate electronic states in the linear arrangement of a polyatomic molecule. The corresponding DFT results are presented in Table II and Figure 6. Let us first discuss Figure 6, which displays the potential energy curves of the singly triplet excited states calculated as a function of the bending angle δ(bz–Ru–bz). It is seen that only the $^3B_2$ state (see E_1) is RT active, while the remaining ones keep their D_{6h} symmetry. The structure of $[Ru(bz)_2]^{2+}$ is bent by around 20° (nonlocal 17°), and the corresponding RT energy is roughly 650 cm^{-1}. The latter value has been defined as the energy difference between the linear and the bent structure. Our findings corroborate the experimental results of Karlen et al.,[3] who have shown that the photochemical ligand substitution proceeds via an associative mechanism. The origin of the difference between potential energy curves of $^3B_2$ (see E_1) and $^3B_1$ (see E_2) is clear. Because the e_{1u} mode splits up $e_{1g} \rightarrow b_1(d_{xz}) + b_2(d_{yz})$, the d_{xz} and d_{yz} orbitals lie in planes that are perpendicular and parallel to the bending mode, respectively. This results in the fact that the interaction between the d_{yz} and the π orbitals of the rings is more affected by the e_{1u} mode than that involving the d_{xz} orbital. The inclusion of the BUP leads to somewhat different results, as shown by Table II. It can be seen that the RT effect vanishes as the crystal packing is taken into account. This result is not surprising, considering that the negatively charged SO_3 groups of two tosylates anions point toward two open faces of $[Ru(bz)_2]^{2+}$.

The most significant result of our investigation is represented in Figure 7a and b, which displays contour levels of the $^1A_1$ and the $^3B_2$ energy as a function of the normal coordinates a_{1g} and e_{1u}. As expected, the potential energy surface (PES) of the ground state exhibits one minimum corresponding to the pseudolinear form.

Let us consider the PES of the $^3B_2$ (see E_1) state. As shown above, its total energy is slightly lowered when $[Ru(bz)_2]^{2+}$ is allowed to relax along e_{1u}. It can be seen on Figure 7b that the system simultaneously undergoes an expansion along a_{1g}

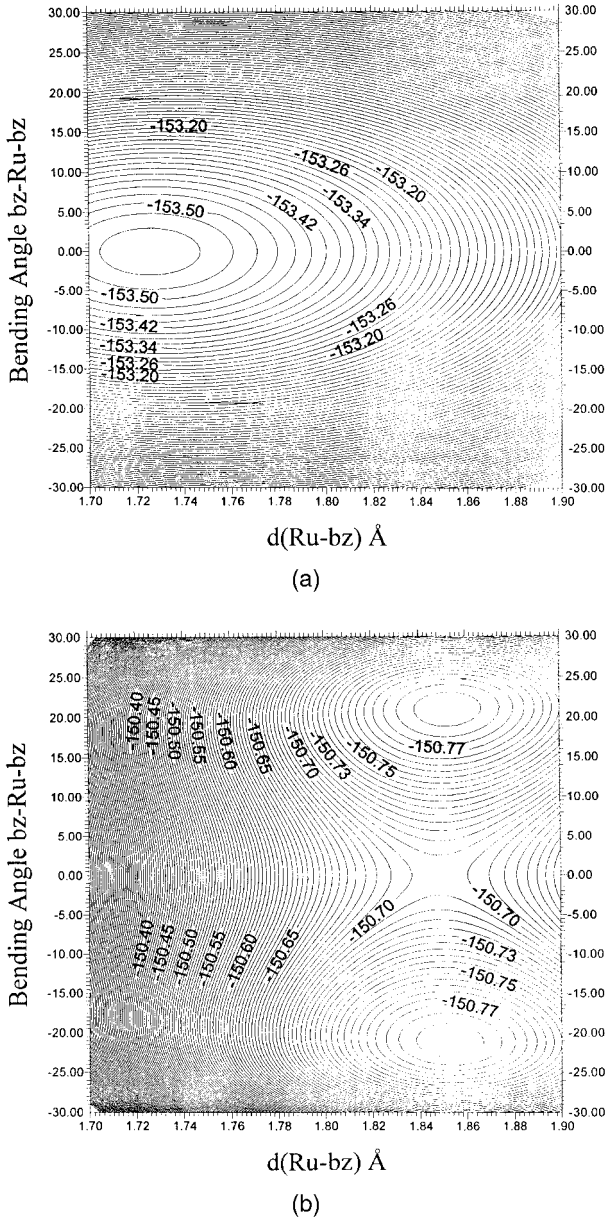

FIGURE 7. (a) Contour plot of the adiabatic potential energy surface of the $^1A_{1g}$ ground state along the a_{1g} and the Q_ε component of the e_{1u} normal coordinates for $[Ru(bz)_2]^{2+}$ in the solid state. (b) As in Figure 7a, but for the E_1 component.

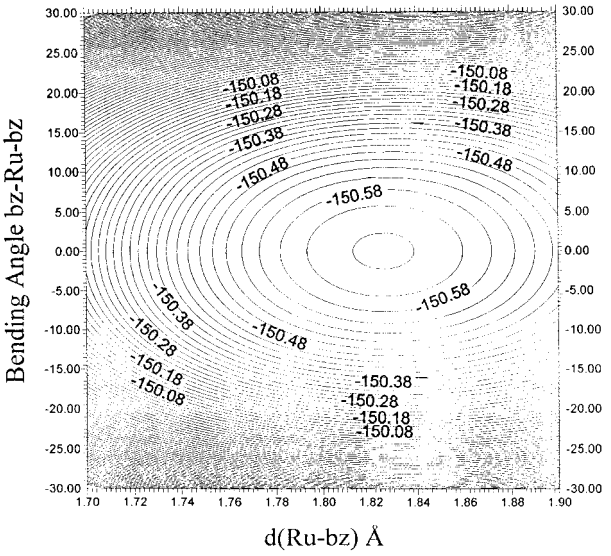

FIGURE 8. As Figure 7a. It can be seen that the Renner–Teller effect is cancelled when including the BUP.

(Δd(Ru–bz) + 0.006 Å) and e_{1u}. The resulting energy stabilization is around 800 cm^{-1}. This result is not surprising, considering the steric hindrance of the rings to each other. As expected, the inclusion of the BUP removes the distortion along e_{1u} and reduces the expansion along a_{1g} as displayed by Figure 8. This behavior is far from the one encountered in crystalline ruthenocene in which the effect of the crystal packing was not strong enough to counterbalance a RT stabilization.[20]

Conclusion

The calculated geometry of the $^1A_{1g}$ ground state of $[Ru(bz)_2]^{2+}$ is in very good agreement with the experimental value. The experimental structural parameters are unfortunately unavailable for the singly excited triplet states, but a similar accuracy may be expected. The photochemical properties are slightly underestimated except for the Stokes shift, for which the agreement is very good. A Renner–Teller distortion along the e_{1u} mode was found, as confirmed by experimental findings. This work shows that a Buckingham potential might very efficiently model the crystal packing. The latter tends to shorten the bond length and hinders the relaxation along e_{1u}. Even considering the overall agreement as fortuitous, the results obtained are very gratifying. This suggests that DF calculations of the type reported here are able to accurately reproduce both structural and photochemical properties of transition metal complexes.

Acknowledgments

The authors are grateful to Professor H. Bill for fruitful discussions. Financial support by the Swiss National Science Foundation is gratefully acknowledged.

References

1. Warren, K. D. Struct Bonding (Berlin) 1975, 27, 45.
2. Beck, U.; Hummel, W.; Buergi, H.-B.; Ludi, A. Organometallics 1987, 9, 20.
3. Karlen, T.; Hauser, A.; Ludi, A. Inorg Chem 1994, 33, 2213.
4. Baerends, E. J.; Ellis, D. E.; Ros, P. Chem Phys 1971, 2, 41.
5. Ravenek, W. Algorithms and Applications on Vector and Parallel Computers; te Riele, H. J. J.; Dekker, Th. J.; van de Horst, H. A.; Eds., Elsevier: Amsterdam, 1987.
6. Boerrigter, P. M.; Te Velde, G.; Baerends, E. J. Int J Chem Quantum Chem 1988, 33, 87.
7. Te Velde, G.; Baerends, E. J. J Comput Phys 1992, 99, 84.
8. Vosko, H. S.; Wilk, L.; Nusair, N. Can J Phys 1980, 58, 1200.
9. Krijn, J.; Baerends, E. J. Fit Functions in the HFS-Method; the Free University of Amsterdam: The Netherlands, 1981.
10. Hohenberg, P.; Kohn, W. Phys Rev B 1964, 136, 864; Kohn, W.; Sham, L. Phys Rev 1965, 140, 1133; Lev, M. Proc Natl Acad Sci USA 1979, 76, 6062; Levy, M. Phys Rev B 1982, 26, 1200.
11. Parr, R. G.; Yang, W. Density-Functional Theory of Atoms and Molecules; Oxford University: New York, 1986.
12. Oliveira, L. N.; Gross, E. K. W.; Kohn, W. Phys Rev A 1988, 37, 2821.
13. Sen, K. D. Chem Phys Lett 1992, 188, 510.
14. Ziegler, T. Can J Chem 1995, 73, 761.
15. Ziegler, T.; Tschinke, V.; Fan, L.; Becke, A. D. J Am Chem Soc 1989, 111, 9177.
16. Ziegler, T. Chem Rev 1991, 91, 651.
17. Coq, B.; Goursot, A.; Tazi, T.; Figuéras, F.; Salahub, D. R. J Am Chem Soc 1991, 113, 1485.
18. Slater, J. C. Adv Quantum Chem 1972, 6, 1.
19. Case, D. A. Annu Rev Phys Chem 1982, 33, 151.
20. Gilardoni, F.; Hauser, A.; Daul, C.; Weber J. J Chem Phys 1998, 109, 1425.
21. Ziegler, T.; Rank, A.; Baerends, E. J. Theoret Chim Acta 1977, 43, 261.
22. Daul, C. J Chim Phys 1989, 86, 703.
23. Daul, C.; Guedel, H. U.; Weber, J. J Chem Phys 1993, 98, 4023.
24. Slater, J. C. The Self-Consistent Field for Molecules and Solids: Quantum Theory of Molecules and Solids; McGraw-Hill: New York, p. 51, vol. 4.

25. Cotton, F. A. Chemical Applications of Group Theory; John Wiley & Sons: New York, 1990.
26. Gilardoni, F.; Weber, J.; Bellafrouh, K.; Daul, C.; Guedel, H. U. J Chem Phys 1996, 104, 7626.
27. Bernhardt, P. V.; Comba, P. Inorg Chem 1992, 31, 2638.
28. Jungwirth, P.; Stussi, D.; Weber, J. Chem Phys Lett 1992, 190, 29.
29. Park, C.; Almlöf, J. J Chem Phys 1991, 95, 1829.
30. Lüthi, H. P.; Ammeter, J. H.; Almöf, J.; Faegri, K. J Chem Phys 1982, 77, 2002.
31. Becke, A. D. J Chem Phys 1988, 88, 2457; Becke, A. D. Phys Rev A 1988, 38, 3098.
32. Perdew, J. P. Phys Rev B 1986, 33, 8822; Perdew, J. P. Phys Rev B 1986, 34, 7046.
33. Pyykkö, P. Chem Rev 1988, 88, 563.
34. Pepper, M.; Bursten, B. E. Chem Rev 1991, 91, 719.
35. Eliav, E.; Kaldor, U.; Ishikawa, Y. Phys Rev A 1994, 49, 1724.
36. Rajagopal, A. K. J Phys C 1978, 11, L943.
37. MacDonald, A. H.; Vosko, S. H. J Phys C 1979, 12, 2977.
38. Engel, E.; Keller, S.; Facco Bonetti, A.; Müller, H.; Dreizler, R. M. Phys Rev A 1995, 52, 2750.
39. Engel, E.; Müller, H.; Speicher, C.; Dreizler, R. M. Density Functional Theory; NATO ASI Series B, Gross, E. K. U.; Dreizerl, R. M.; Eds.; Plenum: New York, 1995, p. 65, vol. 337.
40. Stueckl, A. C.; Daul, C.; Guedel, H. U. Int J Quantum Chem 1997, 61, 475.